PREDICTION OF TRAFFIC-INDUCED VIBRATION IN COMPOSITE GIRDER BRIDGE USING MODAL BASED METHOD

Sakda Chaiworawitkul* Piotr Omenzetter** Masato Abe*** and Yozo Fujino****

* Graduate Student, Dept. of Civil Eng., The University of Tokyo, Hongo, Bunkyo-ku, Tokyo 113-8656

** Ph.D., Postdoctoral Fellow, Dept. of Civil Eng., The University of Tokyo, Hongo, Bunkyo-ku, Tokyo 113-8656

*** Ph.D., Associate Professor, Dept. of Civil Eng., The University of Tokyo, Hongo, Bunkyo-ku, Tokyo 113-8656

**** Ph.D., Professor, Dept. of Civil Eng., The University of Tokyo, Hongo, Bunkyo-ku, Tokyo 113-8656

This study deals with 3-dimensional analytical prediction of traffic-induced vibration in a composite girder bridge as a preliminary approach to environment associated problem, e.g. acoustic emission due to structure-induced vibration generated by traffic load. Based on modal approach, this method benefits on modal information obtained from FEM analysis and is computationally superior than direct FEM analysis in the sense that calculation load can be reduced by truncation in number of modes used in calculation. Comparison between field test results and simulations is performed, and good agreement is confirmed. Consideration on influence of bridge structural characteristics, i.e. bearing and slab stiffness, on response is also conducted in order to examine degree of their importance and contribution to traffic-induced vibration. It is found that such features do affect traffic-induced vibration characteristics and significantly effect on its magnitude.

Key Words: Traffic-induced vibration, 3D composite girder bridge model, Local vibration

1. Introduction

Research on traffic-induced vibration in bridges has received considerable attention for several years. The term 'impact factor' has been used through out the world to describe the dynamic effects of wheel loads on bridges. It provides the sense that the term 'impact factor' suggested that dynamic loading is due solely to the impact action of a wheel. In fact, dynamic loading is a complex interaction between moving vehicles and the structure under observation.

Additionally, in recent years, public concern as to environmental problem has been increased. Traffic-induced vibration associated problems, such as, structure-induced low-frequency noise, which are harmful and deleterious to its surrounding public, are taken more seriously.

Thus, the need for a traffic-induced vibration prediction method that provides information about vibration more in detail has been intensified. Unfortunately, according to scarcity of data, especially comparison between field test and calculation results, contribution of traffic-induced vibration to such environmental problems has been left unclear.

A new trend in bridge structure in Japan is to employ less number of girders but wider girder spacing according to an attempt to reduce construction and maintenance cost. After the Hanshin earthquake in 1995, rubber bearing has been more practically used instead of the stiffer fixed bearing as a measure to provide more ductility to the structure. These are likely to result in lower damping and lower tortional rigidity of the entire structure. As a result, more severe vibration and more contribution of transverse and torsional modes of vibration is possible to occur. Therefore, the structure is more prone to vibration in global manner as well as local manner due to oscillation of structural members, e.g. slab and girder[1]. Consequently, traffic-induced vibration associated problems may appear in more serious way.

Therefore, necessity of clarifying the detail of traffic-induced vibration in actual bridge is increasing. It was found by Memory *et al*[2], that the conventional beam analogy appearing ubiquitously cannot realistically model vehicle-bridge interaction, because it does not allow for the torsional and transverse modes of vibration and can only simulate vehicles traveling along the centerline of a bridge. Therefore, it is worthwhile to investigate the dynamic properties due to the traffic load in more realistic manner to clarify the issues above.

In this study, analytical prediction method of traffic-induced vibration in composite girder bridge using 3D bridge model has been developed. The approach proposed herein comprises 2 major parts. The first half deals with eigen-value analysis employing 3D FEM bridge model to obtain modal information. The second part is concerned with modal analysis using modal information adopted from the first section. Advantage of this prediction method can be succeeded by appropriate truncation of number of modes used in calculation. Therefore, the computation can be considerably less cumbersome than performing direct FEM analysis, while the accuracy is preserved. Another merit is that, unlike in beam analysis, this method also allows arbitrary shape of the bridge and position of the vehicle.

Moreover, comparison of computational and experimental results is conducted in order to verify validity of the approach. Finally, consideration on influences of bridge structural characteristics, e.g. bearing stiffness and slab thickness, on response is also carried out. Demonstration of changing these properties parametrically is pragmatically useful in the sense that it provides one with rough imagination of what extent these elements can affect the structure.

2. Vehicle-Bridge Interaction Equation

Overall schematic flow of this the proposed method is illustrated as a diagram in Fig. 1.

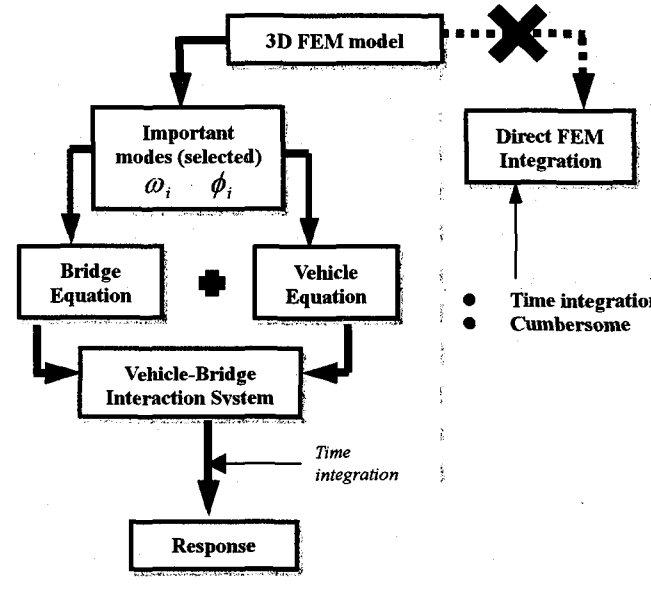

Fig. 1 Study flow

Firstly, the bridge is modeled by Finite Element Method 3-dimensionally. Eigen-value analysis is carried out in order to find modal information, e.g. natural frequencies, modal masses, and mode shapes.

Bridge equation can be established according to the following manner; Displacement of the bridge $\mathbf{u} = \{u_x\ u_y\ u_z\}^T$ at any arbitrary point $\mathbf{x} = \{x\ y\ z\}^T$ can be written in modal form as:

$$u(x,t) = \sum_{n=1}^{\infty} \Phi_n(x) q_n(t) \quad (1)$$

where $\Phi_n = \{\phi_n^x \ \phi_n^y \ \phi_n^z\}^T$ and q_n denote the n-th 3D mode shape and the corresponding generalized coordinate respectively. By assuming proportional damping, the equation of motion of the bridge in generalized coordinates is:

$$\ddot{q}_n(t) + 2\xi_n \omega_n \dot{q}_n(t) + \omega_n^2 q_n(t) = \frac{1}{m_n} \phi_n^z(\mathbf{x}) P(t) \quad (2)$$

where m_n, ξ_n and ω_n represents n-th modal mass, damping ratio and frequency respectively. $P(t)$ denotes the vertical force exerted at point **x** on the bridge.

The vehicle model adopted here is a 2 DOF car model as shown in Fig. 2. Motions of bouncing and pitching which play a key role upon the response can be delineated as in equations (3) - (5).

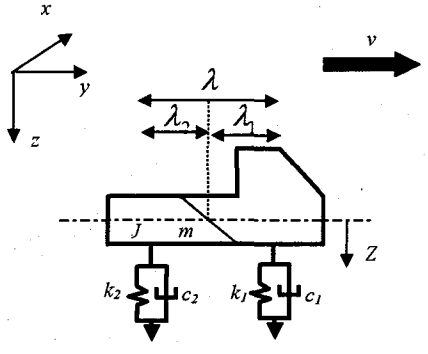

Fig. 2 2 DOF vehicle model

$$m\ddot{Z} + \sum_{i=1}^{2} V_i = 0 \quad (3)$$

$$J\ddot{\theta} - \sum_{i=1}^{2} (-1)^i \lambda_i V_i = 0 \quad (4)$$

$$V_i = \left(k_i + c_i \frac{d}{dt} \right) \left\{ Z - (-1)^i \lambda_i \theta - u_z(\mathbf{x}_i) - r_i \right\} \quad (5)$$

where r_i represents road surface roughness function at the i-th contacting point. V_i in equation (5) serves as an interaction forcing function. Thus, it can be inferred from this mathematical expression that the vehicle equations couple with those of the bridge via Z, vertical direction of the bridge u_z and surface roughness function r_i. Based on this definition of the interaction force V_i, the interaction force function $P(t)$ on the right hand side of the bridge equation (2) can be written as:

$$P(t) = P_1(t) + P_2(t) \quad (6)$$

where

$$P_i(t) = mg \frac{(\lambda - \lambda_i)}{\lambda} - V_i \quad (7)$$

Equation (2), (3), and (4) form vehicle-bridge interaction (VBI) equations. It can be seen that the system of equations is a coupled system expressing interaction between vehicle load and bridge time-dependently. Finally, response of the system can be obtained by operating time integration of equation (2), (3), and (4).

However, the most outstanding merit of this method is that, analogous to that of direct FEM integration, computational load can be truncated effectively by expanding the VBI system equation using only dominant modes. This can accomplish in practice because in general the bridge motion is concentrated in only the first few modes. Additionally, the range of frequency where low-frequency noise problem occurs lies lower than 20 Hz. Therefore, the term 'dominant modes' here can be referred to the range of 0-20 Hz.

3. Experimental Verification

3.1 Field Test

Bridge where the field test was conducted is Hibakaridaira Bridge, constructed and tested by Japan Highway. The bridge is located in Touhokuriku Highway in Gifu Prefecture. It comprises of 4 spans, separated by piers P1-P3, with total length of 193.00 [m]. (47.4 [m] + 48.5 [m] + 48.5 [m] + 47.0 [m]) (See Fig. 3). Supported by 2 rubber bearings at each pier or abutment, the structure cross-section consists of a concrete slab and 2 continuous steel girders (Fig. 4). During experiment, vehicle moved on 3 different routes, i.e. C1, C2, C3 as illustrated in Fig. 5 at constant speed of 30 km/h. Routes C1, C2 and C3 were set as routes of passage over girder 1 (G1), centerline and girder 2 (G2) respectively.

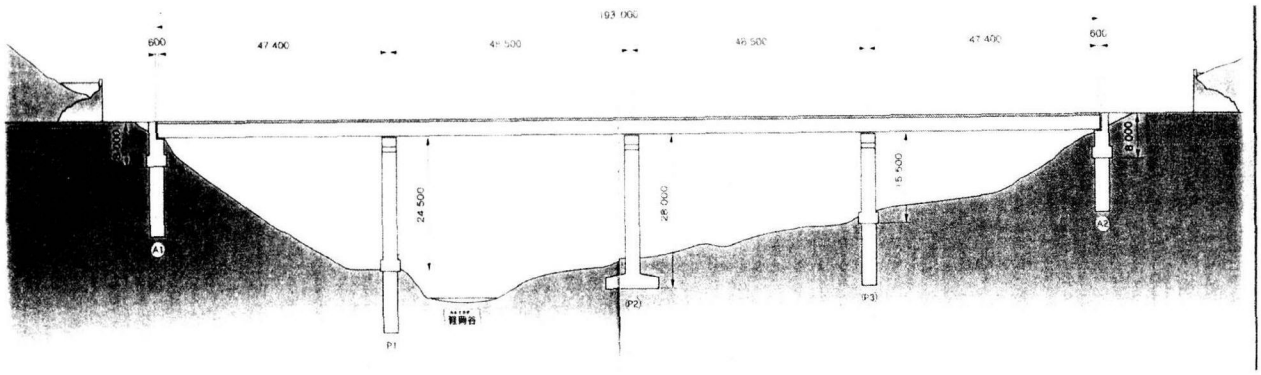

Fig. 3 Elevation of Hibakaridaira bridge

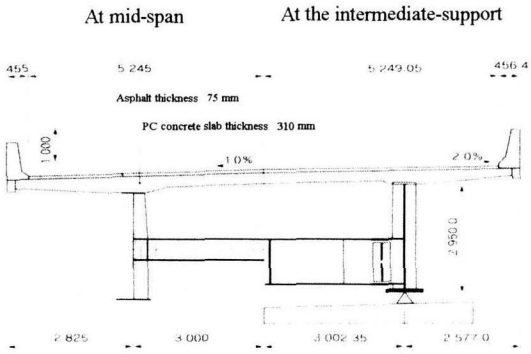

Fig. 4 Cross-section of Hibakaridaira bridge

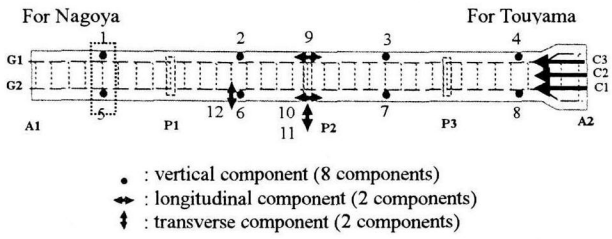

(a) Top view

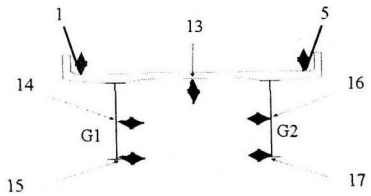

(b) Cross-section

Fig. 5 Measurement setup

Acceleration gauges were located at several points on the slab and on the girders as shown in Fig. 5. Fig. 5 (b) represents the cross-section area at dotted line location in Fig.5 (a).

Measurements started at the moment the vehicle arrived at the middle of the longitudinal length and lasted for 20 seconds.

Drawing of the vehicle used in the experiment and its dimension as well as dynamic properties are as given in Fig. 6 and Table 1 respectively. It is worth noting that the crane comprises comparatively heavy weight, i.e. 36852 [N], while one span of the bridge weighs approximately 1.96e+006 [N].

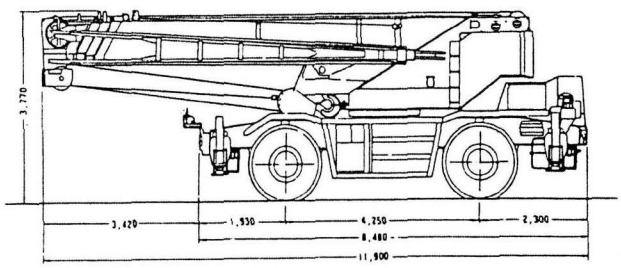

Fig. 6 Vehicle dimension

Table 1 Dynamic properties of the vehicle

Dimension (mm)		**Weight (N)**	
Total length	1220	Total weight	368562
Total height	3650	Front axis	184281
Total width	2990	Rear axis	184281
Wheel base	4820		
Dynamic properties of the vehicle			
Moment of inertia (for bouncing mode)		150900 kg m^2	
Suspension spring constant		736800 N/m	
Suspension damping constant		13518 N/m/s	

3.2 Rubber bearing stiffness

Simplified formulae for determining stiffness of rubber bearing in horizontal and vertical direction are as in equation (8) and (9) respectively[3].

$$K_b = \frac{GA'}{\sum t_e} \tag{8}$$

$$K_c = \frac{EA}{\sum t_e} \tag{9}$$

Where G denotes shear modulus of elasticity, A' denotes effective area of the rubber bearing, $\sum t_e$ denotes sum of rubber slice width, E denotes apparent Young modulus defined by $E = (3+6.58S^2)G$, A is the area of the rubber bearing, S denotes geometrical coefficient of rubber bearing. Based on these formulae, the stiffness values in 3 directions are given as in Table 2:

Table 2 Stiffness values of bearings

	Stiffness [N/m]		
	x-direction	y-direction	z-direction
A1	1.568e+06	1.568e+06	2.834e+09
P1	1.105e+07	1.105e+07	6.242e+09
P2	1.310e+07	1.310e+07	7.439e+09
P3	9.227e+06	9.227e+06	6.242e+09
A2	1.725e+06	1.725e+06	2.772e+09

Here it is worth noting that since the bearings used in Hibakaridaira bridge are of square shapes, the values of their stiffness in horizontal direction, i.e. x- and y- directions, are equal (See Fig. 7).

3.3 Finite Element analysis

Superstructure of Hibakaradaira bridge was modeled by Finite Element in 3 dimensional manner employing 444 shell elements (Fig. 7). Rubber bearings were modeled as linear springs in x-, y-, and z- direction. The value of each bearing stiffness in each direction was given in Table 2. Piers were modeled as springs in 2 horizontal directions corresponding to pier horizontal deflections. (For cross-section of the model, see Fig. 8) whereas abutments were considered as fixed boundaries. Values of stiffness of piers P1-P3 were given in Table 3.

Table 3 Stiffness values of piers

Piers	Stiffness [N/m]		
	x-direction	y-direction	z-direction
P1	1.01e+08	3.74e+08	Fixed
P2	6.00e+07	2.15e+08	Fixed
P3	4.2e+08	1.41e+09	Fixed

The Eigen value analysis was carried out by Kobe Steel Co, Ltd., in order to find modal information, e.g. natural frequencies, and mode shapes, based on the values of the stiffness given in the previous section. Examples of first few modes obtained by the analysis are given in Fig. 9 (a)-(d). Via these results, asymmetry of the mode shapes along bridge axis or along the axis perpendicular to the bridge one can be seen. This is because of the asymmetry of the boundary condition discussed in the previous section. Therefore, as the infeasibility and incapability of the 1D model to cope with asymmetry in shape and position of the structure stated in section 1 are obviously confirmed here, the necessity of 3D model is enhanced correspondingly.

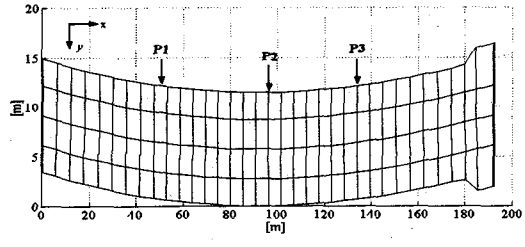

(a) Top view of the slab

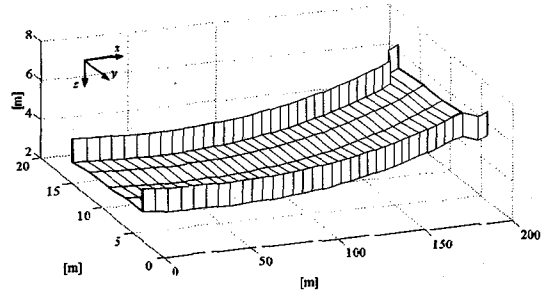

(b) Elevation of the slab

Fig. 7 Meshing of FEM model of superstructure

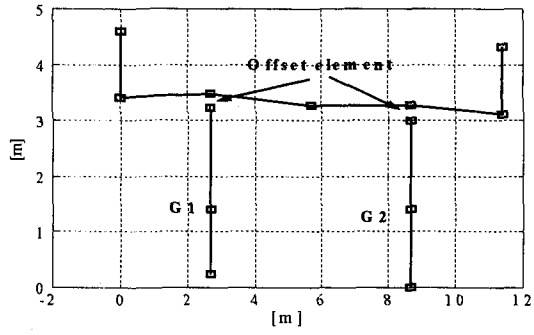

(c) Cross-section

Fig. 7 Meshing of FEM model of superstructure (continued)

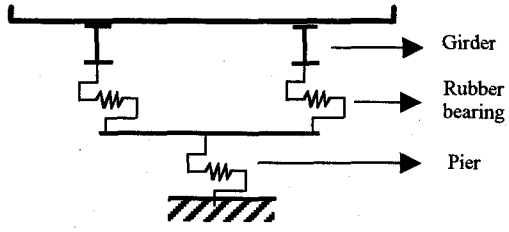

Fig. 8 Cross-section of FEM model

3.4 Comparison

Calculation based on theory in section 2 was conducted in order to reproduce the experimental results. Physical properties of the vehicle are given as stated in Table 1. Modes used here are selected from 0-20 Hz as explained in the theory section and consists of 66 modes. Damping ratio of each mode are assigned based on experimental result report of Japan Highway which states the details as in the following manner.

Table 4 Damping ratio justified for each mode

Experiment	FEM analysis	Mode type	Damping ratio
2.39 Hz	2.36 Hz	1st bending mode	0.011
2.59 Hz	2.57 Hz	1st torsional mode	0.015
2.78 Hz	2.75 Hz	2nd bending mode	0.009
3.56 Hz	3.35 Hz	3rd bending mode	0.007
Otherwise			0.010

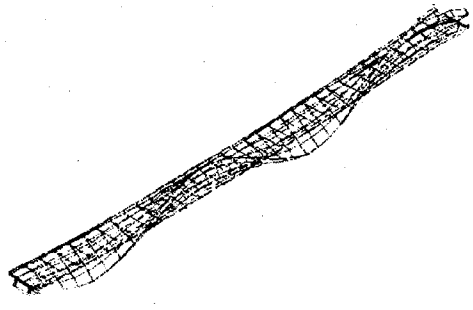

(a) 1st bending mode, 2.36 Hz

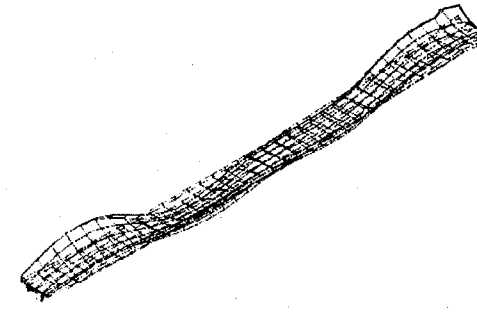

(c) 2nd bending mode, 2.75 Hz

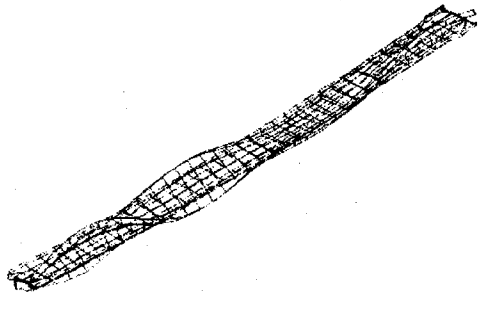

(b) 1st torsional mode, 2.57 Hz

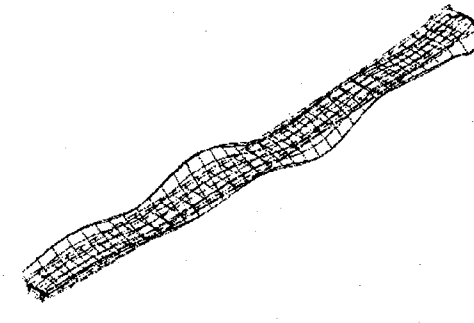

(d) 3nd bending mode, 3.35 Hz

Fig. 9 Examples of mode shapes obtained from FEM

Surface roughness was modeled as a spatial random process whose characteristic is governed by a proper power spectrum, i.e. $S_{z0}(\Omega) = A/(\Omega^2 + \alpha^2)$. Parameter A and α were justified to match good pavement condition in accordance with ISO estimation which are set as 10^{-7} [m^2/(m/c)] and 0.05 [c/m], respectively[4] (see Fig. 10). Sampled irregularity of surface roughness generated based on the power spectrum density function given above is shown in Fig. 11.

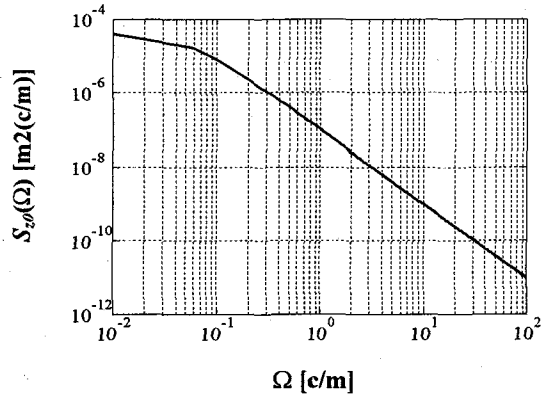

Fig. 10 Power spectrum density function of road surface roughness

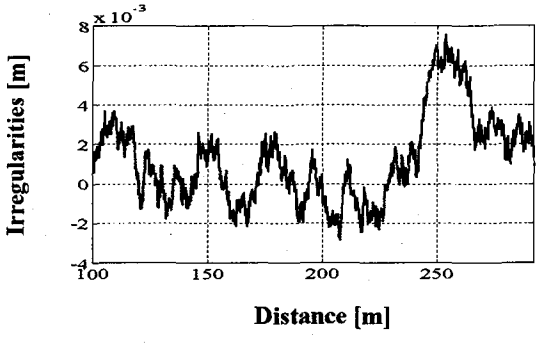

Fig. 11 Sampled irregularities of road surface

For the sake of brevity, only results from case of vehicle running over G1 are shown. Responses from calculation and experiment at points 1, 9, and 14 (Fig. 5) are shown in Fig. 12. Fourier spectral densities (FSD) at the corresponding points are compared in Fig. 13.

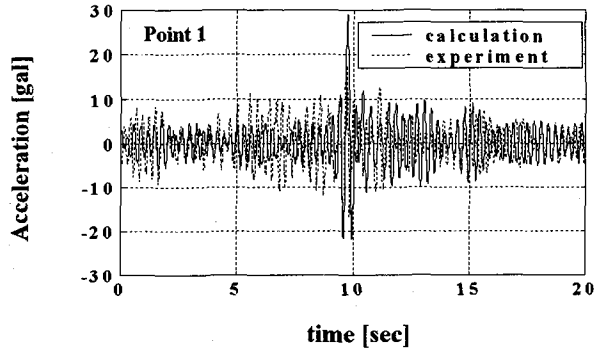

(a) Point 1

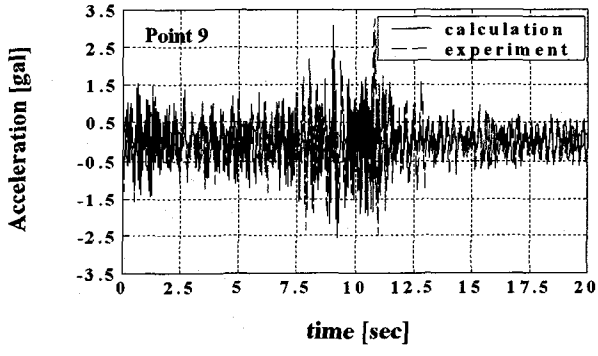

(b) Point 9

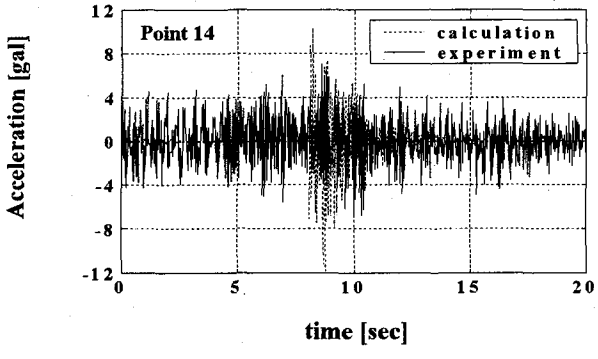

(c) Point 14

Fig. 12 Acceleration responses at point 1, 9 and 14

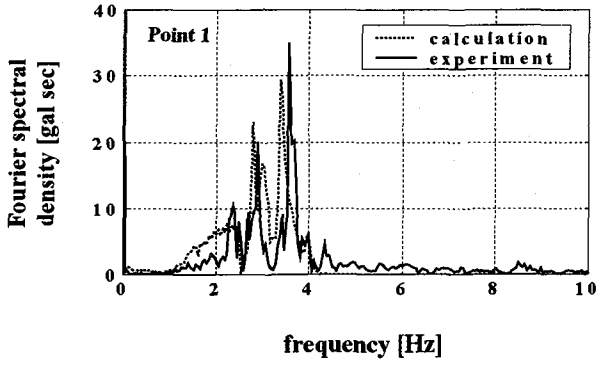

(a) Point 1

Fig. 13 Fourier spectral densites at point 1, 9 and 14

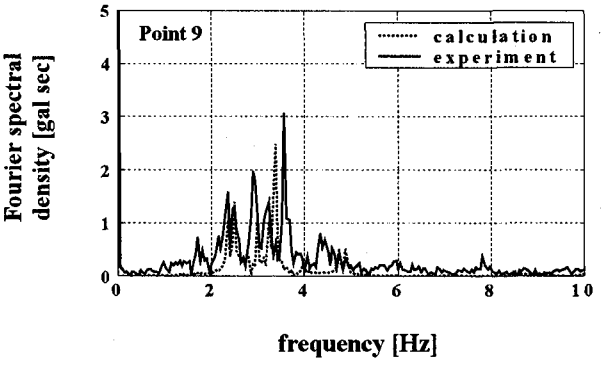

(b) Point 9

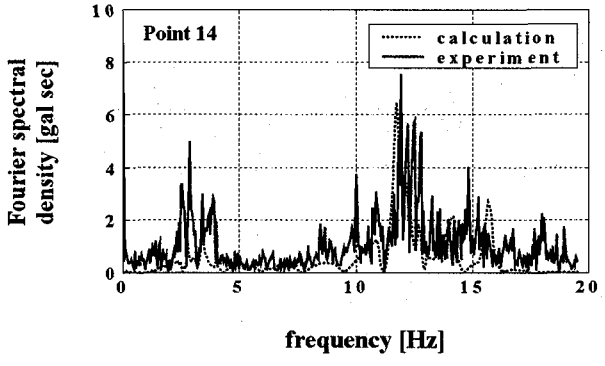

(c) Point 14

Fig. 13 Fourier spectral densites at point 1, 9 and 14 (continued)

Through these figures, reasonable accuracy at a single point of measurement can be observed in terms of magnitude and peak frequency. From the fourier spectral density plots in Fig. 13, for point 1 and 9 located on the slab, 1-3 bending modes are excited (See Table 4). On the other hand, the case of point 14 on the web of girder G1 shows additional peaks between 10-14 Hz. Examples of mode shapes and cross-sectional mode shapes where point 14 located (See Fig. 5 also) are given in Fig. 13. It can be seen from the mode shape pictures that in these modes, rather than vibration in whole scale, vibration in structural elements, such as parapets or girders are more significant.

Based on this information, it can be deduced that global vibration generated in Hibakaridaira bridge is a result of vibration due to modes of frequency 2-4 Hz, whreas 10-14 Hz modes provoke local vibration in the girder and/or plate. Examples of excited mode shapes corresponded to local vibration frequency range, i.e. 10-14 Hz., are shown in Fig. 14.

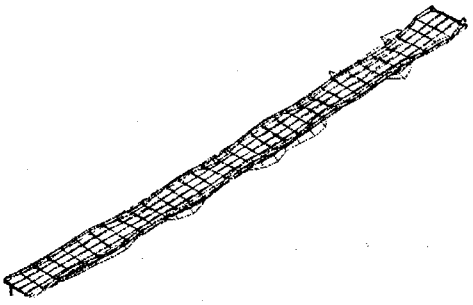

(a) Mode shape at frequency 11.8 Hz

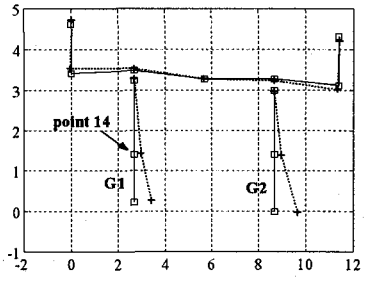

(b) cross-section at point 14, *original (solid line), mode shape at frequency 11.8 Hz (dotted line)*

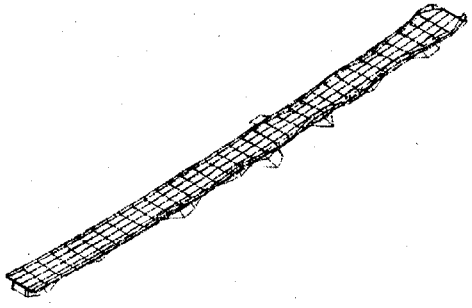

(c) Mode shape at frequency 12.5 Hz

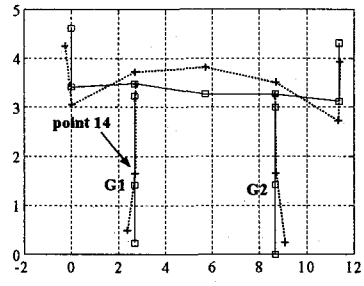

(d) cross-section at point 14, *original (solid line), mode shape at frequency 12.5 Hz (dotted line)*

Fig. 14 Examples of mode shape in the range 10-14 Hz

As an evaluation of prediction accuracy in entire

scale, response standard deviations (SD), defined as:

$$\sigma = \sqrt{\int_0^t (a(t) - \bar{a})^2 dt} \qquad (10)$$

are adopted as a criteria where $a(t)$ and $\bar{a}$ are acceleration response at time t and its mean value respectively. Comparison between calculation results standard deviation values and those from experimental results is shown in Fig. 15 in which, vertical axis shows the standard deviation value of the response at the corresponding measurement point on the horizontal axis. From this plot, good agreement can be observed.

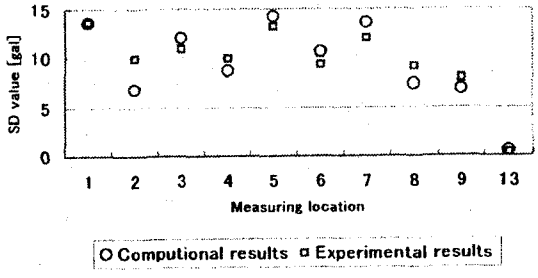

Fig. 15 Prediction method accuracy

Therefore, from the evidence demonstrated above, it can be deduced that the prediction method of traffic-induced vibration using 3D bridge model is successfully established.

4. Parametric study of influence of structural properties on response

In order to clarify effects of structural member properties, such as bearing stiffness or slab thickness, study of influence of structural characteristics on response is conducted parametrically as an application of the prediction method. The following 4 bridge models explained in Table 5 are taken into account.

Modes used in this part are selected from those lying between 0-20 Hz as in the last section similarly for all 4 cases. Modal damping ratio is justified as 0.01 equally for each mode.

Table 5 Models used in parametric study

Model	Superstructure	Bearings
1 (reference)	Hibakaridaira bridge	Rubber (as in section 3.3)
2	Hibakaridaira bridge	Fixed
3	Hibakaridaira bridge	Rubber, 5 times stiffer than in model 1
4	80% Slab thickness compared to model 1	Rubber (as in section 3.3)

Herein, only the case of passage course 1 at point 1, i.e. the point over girder G1, is discussed for the sake of congruency with section 3.4 and insufficiency of space available (See Fig. 5). Response of each case is illustrated in Fig. 16.

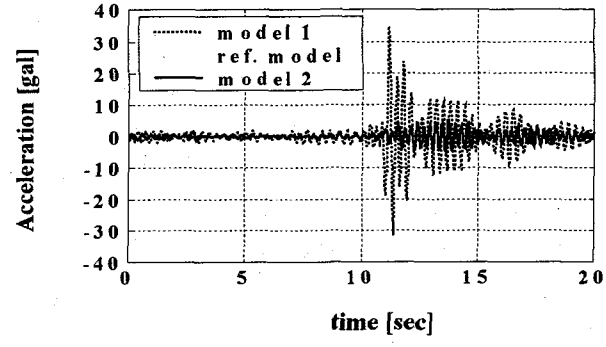

(a) Model 1 and 2

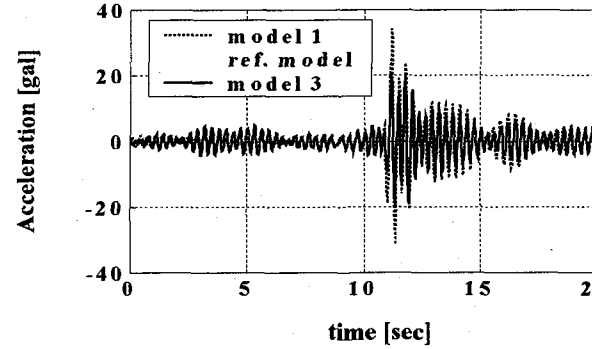

(b) Model 1 and 3

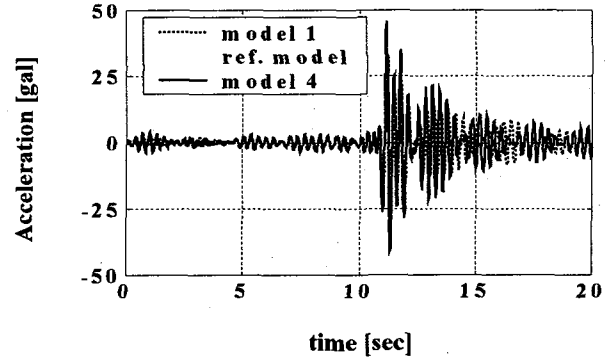

(c) Model 1 and 4

Fig. 16 Comparison of acceleration at point 1

Again, the standard deviation value concept is adopted in order to compare the response magnitudes between two different cases. It is found that:

$$\sigma_2 \approx 0.3\sigma_1 \quad (11)$$

$$\sigma_3 \approx 0.8\sigma_1 \quad (12)$$

$$\sigma_4 \approx 1.2\sigma_1 \quad (13)$$

where σ_i refers to the response standard deviation value of i-th case. The results imply that response can be reduced 20% by increasing stiffness of the bearing by 5 times, whereas using fixed bearings, the response is reduced by approximately 70%. On the other hand, decreasing the slab thickness to 80%, results in 20% increment in the obtained response.

Comparisons of fourier spectral density plots at the same point are shown in Fig. 17. The same trend as in time domain can be found in frequency domain as well. That is, as the structure gets stiffer, the heights of the peaks become smaller, especially peaks in range of 2.5-3 Hz (For more detail, see Table 6-8).

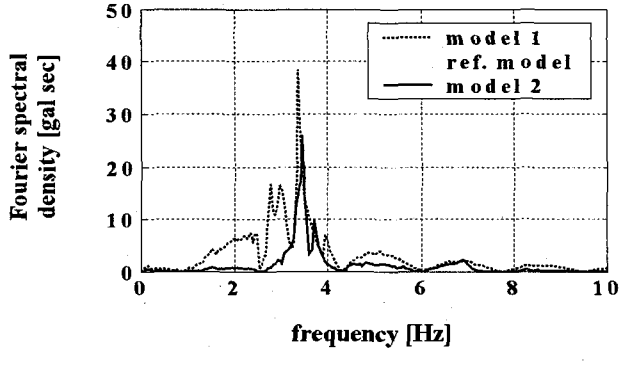

(a) Model 1 and 2

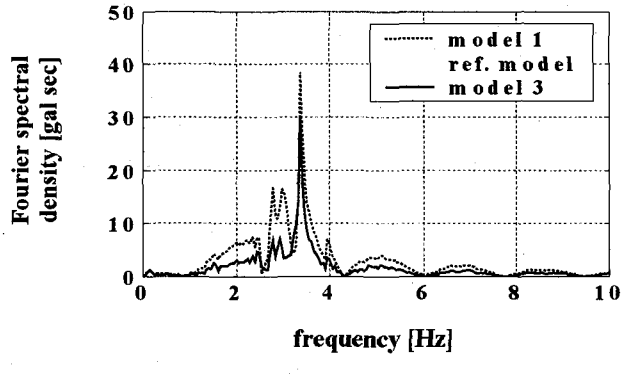

(b) Model 1 and 3

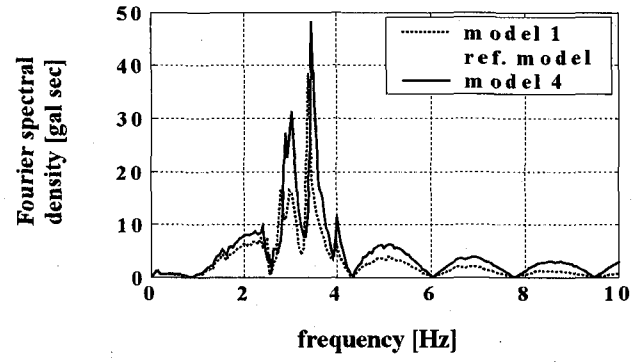

(c) Model 1 and 4

Fig. 17 Fourier spectral density at point 1 of 3 cases

Table 6 Excited modes of model 2

Frequency	Type of mode
3.35 Hz	2nd torsional mode
3.69 Hz	3rd bending mode

Table 8 Excited modes of model 3

Frequency	Type of mode
2.92 Hz	2nd bending mode
3.36 Hz	2nd torsional mode

Table 9 Excited modes of model 4

Frequency	Type of mode
2.40 Hz	1st torsional mode
2.87 Hz	3rd bending mode
2.98 Hz	2nd torsional mode
3.36 Hz	3rd torsional mode

5. Comments on prediction method

Although difficult to identify its exact value, vertical stiffness of a rubber bearing serves as an important value

in boundary condition when solving eigen value problem. Thus occurrence of vibration modes from FEM analysis is vulnerable to this inaccuracy. Therefore, the responses can also be affected accordingly as shown in the following example occurring in this study.

In Fig. 13, one can observe a small lag in peak frequency between calculation result and experimental one. Since the computation shows the peaks in lower frequency range than that of the experimental result, it can be considered that the FEM model is more flexible than the real Hibakaridaira bridge. The most convincing evidence to support this idea is the mode shapes function along the girder G1 where is supported by rubber bearings as shown in Fig. 18. This figure illustrates the 1st bending mode shapes of the original Hibakaridaira bridge. It can be seen from this figure that the value at node number 37 supported by abutment A2 is quite large compared to the maximum value within the same mode, i.e. almost 10 percents of the maximum value.

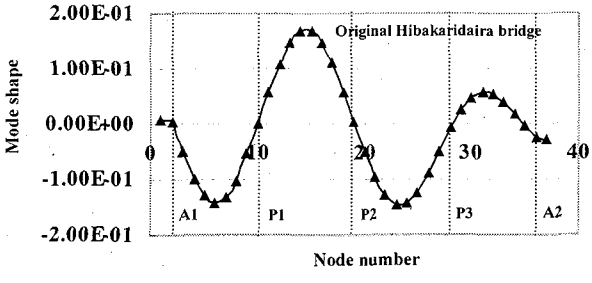

Fig. 18 Underestimation of rubber bearing stiffness

Thus it can be deduced that the values of the stiffness estimated in section 3.2 underestimates the stiffness value of rubber bearing. As a result, the calculation tends to have peaks lying in the lower range of frequency when compared to reality. Even so, the theory proposed here is still valid as one can see from the evidences, such as matching between mode types of the peaks in Fig. 13, or the occurrence of low frequency peaks in softer model, i.e. model 3 and 4, in fourier spectral density plot as shown in Fig. 17.

6. Conclusions

In this study 3D bridge model is introduced a prediction method of traffic-induced vibration problem is proposed. This method is superior to the conventional beam analysis in the sense that it can reproduce behavior of the bridge more realistically without no restriction or limited use. This method is considered to be less time-consuming in term of computational load while accuracy is preserved when compared to direct FEM analysis method. One interesting result is that the difference in term of frequency excited between global and local vibration. Global vibration is provoked in range of 2-4 Hz, whereas those of local vibration lie among 10-14 Hz. Experimental results are compared to computational results and reasonably good agreement is found in both frequency and amplitude. In the second part of this study, parametric study of the influence of structural parameters on response is conducted. It can be concluded from this part that structural characteristics, such as, bearing stiffness or slab thickness, significantly influence on responses of traffic-induced vibration.

Finally, rubber bearing vertical stiffness is practically difficult to estimate. Thus it is likely capable of being a main reason to reduce the prediction accuracy. Therefore, deliberate concern of this issue is crucial and incumbent.

7. Acknowledgement

The second author was supported during this research by the Japan Society for the Promotion of Science Postdoctoral Fellowship for Foreign Researchers in Japan. Computation of the natural modes of the bridge was made by Kobe Steel Co, Ltd. Dr. Nakagawa's cooperation is deeply appreciated. Finally thanks are extended to Mr. Mizuguchi (JH, Nagoya) for data supply, Fuji Engineering Ltd. for many useful information and Dr. K. Kimura (KIT) for his kindness and support.

8. References

1) Nishioka, Tanaka, Inspection of rubber bearing

behavior characteristics, *1997 Colloquium on Bridge Vibration*, pp. 139-146, 1997

2) Memory, T.J., Thambiratnam, D.P. and Brameld, G.H., Free Vibration Analysis of Bridges, *J. Engng Struct.*, 17(10), pp. 705-713, 1995

3) Japan Road Association, *Handbook for bearing design*, 1991

4) Kawatani M. and Komatsu S., Nonstationary random response of highway bridges under a series of moving vehicles, *Proc. Of JSCE*, Structural Eng./Earthquake Eng. Vol. 5, No. 2, 1998

5) Chaiworawitkul S., High Accuracy Prediction of Traffic-induced Vibration in Composite Girder Bridge, Bachelor thesis, The University of Tokyo

6) Chaiworawitkul S., Omenzetter P. and Fujino Y., Prediction of traffic-induced vibration using 3D bridge model and consideration on influence of bridge structural properties on response, *Proceedings of the Second International Summer Symposium*, International Activities Committee Japan Society of Civil Engineers, pp. 9-12, 2000

(Received September 14,2000)